MURDOCH RESEARCH REPOSITORY

This is the author's final version of the work, as accepted for publication following peer review but without the publisher's layout or pagination. The definitive version is available at
http://dx.doi.org/10.1007/s00339-013-7567-9

Jennings, P., Jiang, Z-T, Wyatt, N.M.W., Parlevliet, D., Creagh, C., Yin, C-Y, Widjaja, H. and Mondinos, N. (2013) Characterization of silicon nanowires grown on silicon, stainless steel and indium tin oxide substrates. Applied Physics A, 113 . pp. 723-728

http://researchrepository.murdoch.edu.au/13213/

Copyright: © Springer-Verlag Berlin Heidelberg 2013
It is posted here for your personal use. No further distribution is permitted.

Characterization of Silicon Nanowires Grown on Silicon, Stainless Steel and Indium Tin Oxide Substrates

Philip Jennings [a], Zhong-Tao Jiang [a,*], Nicholas M. W. Wyatt [a], David Parlevliet [a], Christine Creagh [a], Chun-Yang Yin [b], Hantarto Widjaja [a] and Nick Mondinos [a]

[a] School of Engineering and Energy, Murdoch University, Murdoch, 6150 WA, Australia.

[b] School of Chemical and Mathematical Sciences, Murdoch University, Murdoch, 6150 WA, Australia

* Corresponding author: Tel.: +61 8 9360 2867; Fax: +61 08 9360 6346; Email: Z.Jiang@murdoch.edu.au (Zhong-Tao Jiang)

Abstract

Silicon nanowires (SiNWs) have been grown on crystalline silicon (Si), indium tin oxide (ITO) and stainless steel (SS) substrates using a gold catalyst coating with a thickness of 200 nm via pulsed plasma-enhanced chemical vapor deposition (PPECVD). Their morphological, mineralogical and surface characteristics have been investigated using scanning electron microscopy (SEM), X-ray diffraction (XRD), X-ray photoelectron spectroscopy (XPS) and Raman analysis. SiNWs growth is accompanied by oxidation, thus yielding partially (SiO_x) and fully oxidized (SiO_2) Si sheaths. The mean diameters of these SiNWs range from 140 to 185 nm. Si with (111) and (220) planes exists in SiNWs grown on all three substrates while Si with (311) plane is detected only for Si and ITO substrates. Computational simulation using density functional theory (DFT) has also been conducted to supplement the experimental Raman analyses for crystalline Si and SiO_2. XPS results reveal that *ca* 30% of

the SiNWs have been oxidized for all substrates. The results presented in this paper can be used to aid selection of appropriate substrates for SiNW growth, depending on specific applications.

Keywords: Silicon nanowires, PPECVD, XPS, XRD, Raman analysis, density functional theory.

1. Introduction

The favorable electronic properties of silicon (Si) have been thoroughly documented and widely applied in various industrial processes, especially for the manufacture of electronic devices. Even though it has long been indispensable in the microelectronics industry, demand for smaller dimension devices will soon reach beyond the bulk Si limit of size reduction [1]. Silicon nanowires (SiNWs) exhibit high surface to volume ratio and, as such, they exhibit favorable opto-electronic, chemical and mechanical properties compared with bulk Si [2]. The combination of the possibility of integrating SiNWs with pre-existing technologies and infrastructure, as well as the demand for lower dimensionality devices, has piqued the interest of numerous solid state physics research groups worldwide.

SiNW research is a semi-mature field, with studies being conducted as early as 1964 [3] but new characterization and manufacturing technologies have afforded new research opportunities half a century later. The bulk of recent studies on SiNWs are centred on their increasingly small diameters [4-6] and their integration into micro/nano electronic [7] or photovoltaic [8] devices.

One of the most widely used methods to fabricate SiNWs is the vapor–liquid–solid (VLS) method via chemical vapor deposition (CVD) where a metal catalyst locally assists the deposition of the growth precursors and thereby drives the nucleation and growth of the NWs [9,10]. In a CVD process, the selection of substrate influences SiNW growth, since they grow with a preferred orientation if the substrate is epitaxially clean. Using the plasma-enhanced (PE) technique increases the deposition rate and reduces the substrate temperature efficiently.

Crystalline silicon is one of the most popular substrate materials for growing SiNWs via CVD as evidenced by previously reported studies [11,12]. There is an electronic structure dependence of SiNWs on size [5] and oxide sheath [13] which may be reflected in the density of states (DOS) for the NWs analyzed. In this study, SiNWs were grown *en masse* on three

different substrates, namely crystalline silicon (c-Si), indium tin oxide (ITO) and stainless steel (SS) using a gold catalyst via pulsed plasma-enhanced chemical vapor deposition (PPECVD). ITO was studied as a substrate because of its good electrical conductivity and optical transparency pointing to potential applications as a solar cell component while the SS substrate was investigated because it has a boundary structure that lies in between that of semiconducting and conducting materials. Characterizations of the SiNWs, with the three different substrates, were conducted using scanning electron microscopy (SEM), X-ray diffraction (XRD), X-ray photoelectron spectroscopy (XPS) and Raman analysis. Such comparative characterization is useful as it affords an understanding of the physical properties of different substrates utilized in different SiNW applications. The significance of the study is demonstrated by the utilization and subsequent characterization of three substantially different common substrate materials for SiNW growth which, to the best of the authors' knowledge, have not been previously reported in the open literature.

2. Experiment details

2.1 SiNWs grown on different substrates

SiNWs were synthesized using PPECVD at 345ºC. Details regarding this synthesis process can be sourced from our previous report [14]. Silane was used as a silicon source. The sample was allowed to heat up under 3.0 torr of argon for 35 min and for a further 35 min under the mixture of reactant gases. The silicon nanowires were produced using silane mixed with diborane (1% in argon) with 70% silane and plasma duration of 40 s. This allows time for the eutectic droplet formation prior to the plasma enhanced growth process. The SiNWs were grown on crystalline silicon (c-Si), indium tin oxide (ITO) coated corning glass and stainless steel (SS) substrates using a gold catalyst (thickness = 200 nm) as described by

the Wagner and Ellis' classic VLS mechanism [15]. Prior to the deposition process, the substrates were cleaned in an ultrasonic bath using decon-90, ultra-pure water and isopropanol. They were then dried using high purity nitrogen before being transferred into a vacuum system for deposition of the gold catalyst layer. The vacuum chamber base pressure was within 10^{-6} to 10^{-5} torr while the working pressure was 10^{-4} torr. The sample temperature was derived from a thermocouple attached to the top electrode and heater block using measurements via a series of calibrated tests.

2.2 Characterization

Raman spectroscopy analysis was conducted using the ISA (Dilor) Dispersive Raman spectrometer with a HeNe 632 nm laser using the 600 and 1800 grating settings. A D3 filter (laser power *ca* 3.3 μW) was used with a data collection time of 100 s. X-ray diffraction (XRD) spectra were collected using a Bruker D8 Advance diffractometer with the *Lynx* Eye detector operating at 2θ step size of 0.0389° and tube voltage and current of 40 kV and 40 mA, respectively.

Surface morphology of the samples was examined using a PHILLIPS XL 20 scanning electron microscope (SEM). The samples were analysed without any additional gold coating so that the morphology of the nanowires could be observed in detail. Mean SiNW diameters were calculated using a Digital Micrograph (Gatan Software Team 1999).

X-ray photoelectron spectroscopy (XPS) analysis was conducted using the Kratos Axis Ultra XPS spectrometer (Manchester, UK) with Mg Kα radiation (hv = 1253.6 eV). The sample was mounted horizontally on the holder and normal to the entrance of the electrostatic lens. Base pressure of the analyser chamber was maintained at ~10^{-9} torr. The voltage and emission current of the X-ray source were kept at 12 kV and 12 mA, respectively. The pass energy was set to 80 eV for the survey scan and 10 eV for the features of interest (i.e., Si 2p,

Si 2s, O 1s and C 1s) to ensure high resolution and good sensitivity. The XPS spectra energy scale was calibrated using Cu $2p_{3/2}$ (932.67 eV), Ag $3d_{5/2}$ (368.27 eV), C 1s (284.6 eV) and Au $4f_{7/2}$ (83.98 eV). The electrostatic lens mode and analyzer entrance were selected in the Hybrid and Slot modes (Iris = 0.6 and Aperture = 49), respectively. A charge neutralizer was employed during the XPS measurements. The gold layer was characterised by using XRD and XPS as references. This layer was established by the binding energy of Au4f7/2 at 84 eV and the observation that 2θ of Au (111) was at 38.2° (the wavelength of x-ray source was 1.5406 x 10^{-10} m).

3. Results and discussion

The SiNWs appear to be highly crystalline (Fig. 1) with wires exhibiting 'kinking' defects [14] instead of amorphous 'worm-like' defects. Mean diameters of the SiNWs, when a 200 nm thick gold catalyst layer was used, are indicated in Table 1 and range from 140 nm to 185 nm for all the substrates used. It is clearly seen that the average wire diameter increases through the following sequence: c-Si → SS → ITO. Observation of "droplets" on the tip of the nanowires is archetypal of the VLS mechanism [15] in which they ride atop the nanowires during the growth process. It appears that there are marginal morphological differences between the SiNWs grown on the three substrates, although nanowires on c-Si and SS are denser and exhibit more homogeneous sizes compared to ITO.

Fig. 2 shows the XRD spectra of the SiNWs on c-Si, ITO and SS substrates. Closer inspection of each spectrum with TOPAS (BrukerAXS 2007) and peak identification using Inorganic Crystal Structures Database (JCPDS 1999) enabled identification of various crystalline structures. The crystalline Si system is cubic with space group $Fd\bar{3}m$(227) (a = 5.43086(3) (JCPDS-89-5012)). Crystalline Au (gold catalyst) with (111) plane is detected at 38.5º (JCPDS-01-1174) for c-Si and SS substrates while there is no clear evidence of such

crystalline gold from the ITO substrate. Iron with (110) and (111) orientations was detected at 44.1º and 45.0º, respectively for the SS substrate (JCPDS-01-1252/88-2324). Consistent with the VLS mechanism [15], the highly crystalline Si (111) plane corresponds to the sharp peak at 28.5º and exists on all three substrates. However, it is interesting to note that the Si (311) plane is detected at *ca* 56.4º for Si and ITO substrates (JCPDS-89-5012) while the Si (220) plane is detected on all three substrates (at 47.5°) albeit with relatively pronounced peak broadening. This peak broadening implies that the Si (220) crystallites are comparatively smaller than the Si (111) and (311). The three main Si plane orientations, (111), (220 and (311), have been reported in previous studies of SiNW deposition [16,17].

SiO_2 is invariably formed via oxidation of Si upon exposure in air [18]. Prominent peaks, *ca* 22.5° and 34.3º, can be assigned to tetragonal (101) and cubic (111) forms of SiO_2 with space groups $P4_12_12(92)$ (a = 4.96, c = 6.68) and $Fm\bar{3}m(225)$ (a = 4.52), respectively (JCPDS-89-3606/3609). It is interesting to note that no tetragonal form of SiO_2 is detected with the c-Si substrate, while the cubic form of SiO_2 is observed in all three substrates with a very weak peak identified with the c-Si substrates. The SiNWs on the c-Si substrate are barely oxidised whilst those on the ITO and SS are considerably oxidised and predominantly in the tetragonal form of SiO_2. The observed increase in SiNWs thickness (Table 1) from c-Si to ITO substrates is due to the oxide coating of the SiNWs. This is reinforced by the observed increase of the total integrated area of all the SiO_2 peaks from XRD spectra (Fig. 2) which shows that the SiO_2 layer increases through the following sequence: c-Si $\rightarrow$ SS $\rightarrow$ ITO. A similar pattern is seen in the density (see Fig. 1) and the thickness of SiNWs (see Table 1).

As shown above, atmospheric oxygen has not oxidized the SiNWs on the c-Si substrate in any significant amount. It may well be that the oxygen needed for significant SiO_2 to form on SINWs from ITO and SS substrates comes from oxygen attached (chemically or physically) to the substrates. The presence of SiO_2 is a notable aspect in the study of SiNWs for opto-

electronic applications since light trapping efficiency of SiNWs shielded with semiconducting and insulating materials (e.g. SiO_2, SiC or SiN) is essentially enhanced via anisotropic light propagation [19].

XRD identification of crystalline Si and SiO_2 implies the possibility of development of Si/SiO_2 core-shell structure as a result of oxidation [20]. Interplanar spacing (*d*) was calculated for Si (JCPDS-89-5012) by first determining the lattice parameter, *a*, and using this to determine *d* via equations (1) and (2):

$$a = \frac{\lambda\sqrt{h^2 + k^2 + l^2}}{2\sin\theta} \tag{1}$$

$$d = \sqrt{\frac{a^2}{h^2 + k^2 + l^2}} \tag{2}$$

Crystallite size was estimated using the TOPAS (BrukerAXS 2007) integral breadth algorithm with a unit Scherrer constant. Fig. 3 shows the Si crystallite sizes with respect to (111), (220) and (311) orientations and substrates used. It is evident that SiNWs grown on the SS substrate generally possess smaller crystallite sizes (< 100 nm diameter) compared with the other two substrates.

Fig. 4 shows the normalized Raman spectra of the SiNWs on Si, ITO and SS substrates. These spectra appear to be qualitatively similar. The sharp peaks at 519 cm^{-1} detected on all substrates confirm the presence of crystalline Si which is also reported by Zhang and co-researchers [18]. The relatively broadened peaks observed *ca* 480 cm^{-1} for all substrates are representative of oxidized Si [18].

In order to interpret the experimental Raman data, a computer simulation was conducted for crystalline Si with space group $Fd\bar{3}m$(227) and lattice parameter 5.43086 Å as well as SiO_2 with space group $Fm\bar{3}m$(225) and lattice parameter 4.52 Å. The simulation was

executed using density functional theory (DFT) enabled by Gaussian 09W software with the following stipulation: B3LYP functional, 3-21G basis set, singlet state and 2 unit cells. Crystalline Si is passivated with hydrogen. Initial calculations confirmed that these parameters provided the lowest ground state energy. Subsequent calculations were made to simulate the Raman spectra for crystalline Si and SiO_2 (Fig. 5). The simulated major peak intensities of crystalline Si and SiO_2 are at 490 and 411 cm^{-1}, respectively, which are within 5-14 % of the experimental peaks Also, the second highest peak intensity for the simulated crystalline Si Raman spectrum at around 900 cm^{-1} is fairly consistent with the experimental Raman spectrum (Fig. 4). That said, however, it is acknowledged that our simulation results are not intended to be an absolute representation of the experimental results and that the former should only be used as an approximate guide. This is especially so in the context where SiO_2 detected in SiNWs may also represent partially oxidized suboxides (amorphous SiO_x) which are not considered in our simulation.

Fig. 6 shows the XPS spectra of the Si nanowires on the three substrates with curve-fitting of the Si 2p envelope. The Si 2p peak was fitted with a doublet spacing constraint of 0.6 eV and a 1:2 intensity ratio via Tougaard backgrounds with Si parameters (CasaSoftware 2001). The decoupling of Si 2p consists of three silicon components, i.e., (1) crystalline Si (2) SiO_2 and (3) SiO_x in the order of decreasing atomic percentages. The detection of amorphous SiO_x implies its presence as a coating component (sheath) of the crystalline Si core along with SiO_2 [21] and this substantiates the Raman spectroscopic results.

It is clear from the XPS spectra that *ca* 30% of the SiNWs surfaces have been oxidized in all substrates. The apparent inconsistency of the SiO_x/SiO_2 ratios between the XPS, XRD and Raman arises because XPS is a surface analysis technique while XRD and Raman provide bulk structural information. Although the XRD results for c-Si substrate indicate insignificant

amounts of silicon oxides, the XPS spectra indicate that these are predominantly on the surface of the material.

The ratio of silicon oxide forming on the surface of SiNWs is related to the amount of crystalline Si and as such, a larger wire will be able to support more oxide sheath on the surface. There is no qualitative difference between the three XPS spectra although the percentage of fully oxidized Si (SiO_2 shell) compared to the partially oxidized SiO_x is the highest for SiNWs grown on the SS substrate followed by ITO and Si substrates.

4. Conclusions

SiNWs have been grown on Si, ITO and SS substrates using a gold catalyst via pulsed plasma-enhanced CVD and duly characterized using SEM, XRD, XPS and Raman analyses. In all cases, the SiNW growth is consistent with the classic VLS mechanism and characterization results indicate the occurrence of oxidation, thus yielding partially (SiO_x) and fully oxidized (SiO_2) Si sheaths. The XRD, Raman and DFT simulation clearly show the considerable silicon oxides layer on the SiNWs prepared on the SS and ITO substrates. The surface characteristics of the SiNWs are similar for all substrates. The morphological characteristics differ in the density, thickness and oxide sheath of the synthesised SiNWs. The crystallite diameters of SiNWs grown on ITO were ~20% larger than those grown on c-Si and SS. This appears to be due to a thicker SiO_2 coating on SiNWs grown on ITO substrates. The SiNWs grown on the different substrates had quite different structural characteristics. These characterization results have technological implications as they indicate how important it is to select the appropriate substrates for SiNW growth depending on the intended applications.

Acknowledgments

This research project was financially supported by Murdoch University Research Institute Strategic Research Fund 2009.

References

[1] A.K. Singh, V. Kumar, Y. Kawazoe, in Nanosilicon, (Elsevier Ltd, UK, 2007).

[2] R.P. Wang, G.W. Zhou, Y.L. Liu, S.H. Pan, H.Z. Zhang, D.P. Yu, Phys. Rev. B **61,** 16827 (2000).

[3] R.S. Wagner, W.C. Ellis, K.A. Jackson, S.M. Arnold, J. Appl. Phys. **35,** 2993 (1964).

[4] S. Hofmann, C. Ducati, R.J. Neill, S. Piscanec, A.C. Ferrari, J. Geng, R.E. Dunin-Borkowski, J. Robertson, J. Appl. Phys. **94**, 6005 (2003).

[5] X. Zhao, C.M. Wei, L. Yang, M.Y. Chou, Phys. Rev. Lett. **92**, 236805 (2004).

[6] I. Ponomareva, M. Menon, E. Richter, A.N. Andriotis, Phys. Rev. B **74,** 125311 (2006).

[7] Y. Cui, Z. Zhong, D. Wang, W.U. Wang, C.M. Lieber, Nano Lett. **3**, 149 (2003).

[8] K. Peng, X. Wang, S.T. Lee, Appl. Phys. Lett. **92,** 163103 (2008).

[9] H. Griffiths, C. Xu, T. Barrass, M. Cooke, F. Iacopi, P. Vereecken, S. Esconjauregui, Surf. Coat. Technol. **201,** 9215 (2007).

[10] I. Zardo, S. Conesa-Boj, S. Estradé, L. Yu, F. Peiro, I. Roca, P. Cabarrocas, J.R. Morante, J. Arbiol, I. Fontcuberta, A. Morral, Appl. Phys. A **100**, 287 (2010).

[11] H. Hamidinezhad, Z. Abdul-Malek, Y. Wahab, Appl. Phys. A **108,** 739 (2012).

[12] A.A. Yasseri, S. Sharma, T.I. Kamins, Z. Li, R.S. Williams, Appl. Phys. A **82,** 659 (2006).

[13] R.J. Bondi, S. Lee, G.S. Hwang, ACS Nano **5**, 1713 (2011).

[14] D. Parlevliet, P. Jennings, J. Nanopart. Res. **13**, 4431 (2011).

[15] R.S. Wagner, W.C. Ellis, Appl. Phys. Lett. **4,** 89 (1964).

[16] J. Niu, J. Sha, Y. Wang, X. Ma, D. Yang, Microelec. Eng. **66**, 65 (2003).

[17] X.-Y. Zhang, L.-D. Zhang, G.W. Meng, G.-H. Li, P.N.Y. Jin, F. Phillip, Adv. Mater. **13**, 1238 (2001).

[18] Y.F. Zhang, Y.H. Tang, N. Wang, D.P. Yu, C.S. Lee, I. Bello, S.T. Lee, Appl. Phys. Lett. **72,** 1835 (1998).

[19] B.S. Swain, B.P. Swain, N.M. Hwang, Mater. Chem. Phys. **129,** 733 (2011).

[20] V.A. Sivakov, R. Scholz, F. Syrowatka, F. Falk, U. Gosele, S.H. Christiansen, Nanotechnol. **20,** 405607 (2009).

[21] S. Kim, C.O. Kim, D.H. Shin, S.H. Hong, M.C. Kim, J. Kim, S.H. Choi, T. Kim, R.G. Elliman, Y.M. Kim, Nanotechnol. **21**, 205601 (2010)**.**

Figure captions

Fig. 1. SEM micrographs of SiNWs grown on (a) Si substrate; (b) SS substrate; and (c) ITO substrate with a 200 nm thick gold catalyst layer.

Fig. 2. XRD spectra of SiNWs on Si, SS and ITO substrates.

Fig. 3. Crystallite sizes. Si(311) was not detected on the SS substrate.

Fig. 4. Normalized Raman spectra of Si and SiNWs on Si, SS and ITO substrates.

Fig. 5. Simulated Raman spectra of (a) crystalline Si; and (b) SiO_2. Insets illustrate the corresponding unit cells used in the simulation.

Fig. 6. XPS spectra of the Si nanowires on the three substrates with curve-fitting of the Si 2p envelope. Dashed lines correspond to fit envelopes.

Table 1 Average diameter of SiNWs (200 nm gold coating thickness)

Substrate	Mean Diameter (nm)	Standard Deviation (± nm)
c-Si	140	47
SS	146	42
ITO	185	115

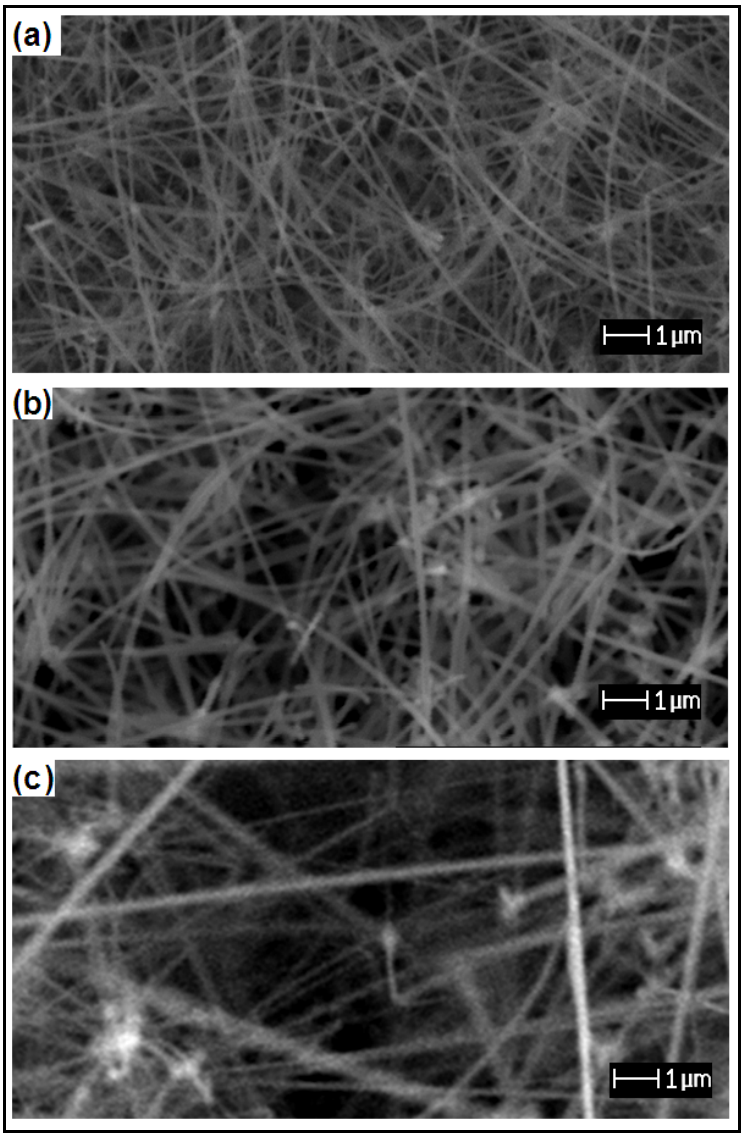

Fig. 1.

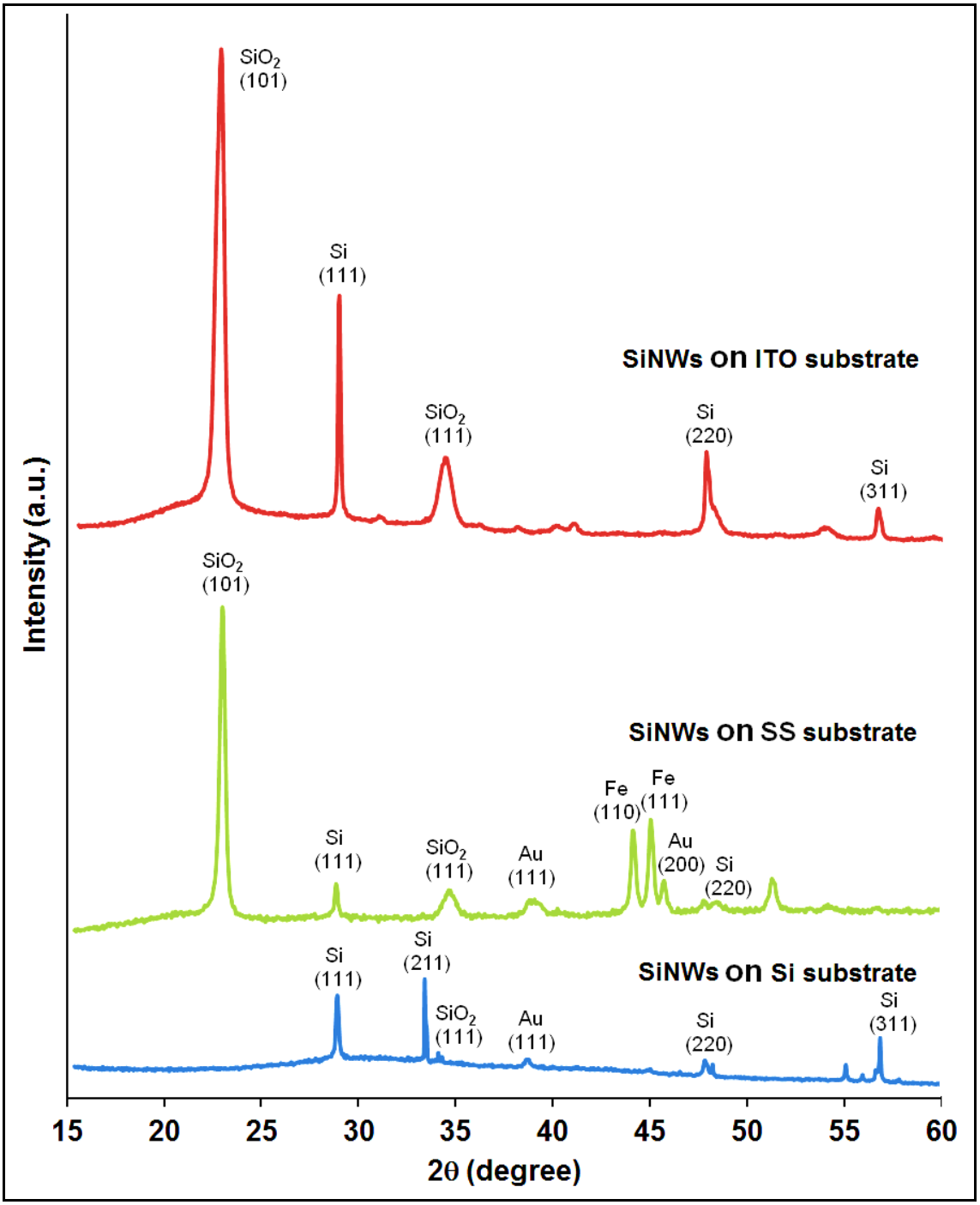
SiO2 (101)
Si (111)
SiNWs on ITO substrate
SiO2 (111)
Si (220)
Si (311)
SiO2 (101)
SiNWs on SS substrate
Si (111)
SiO2 (111)
Au (111)
Fe (110)
Fe (111)
Au (200)
Si (220)
Si (111)
Si (211)
SiNWs on Si substrate
SiO2 (111)
Au (111)
Si (220)
Si (311)
Intensity (a.u.)
15
20
25
30
35
40
45
50
55
60
2θ (degree)

Fig. 2.

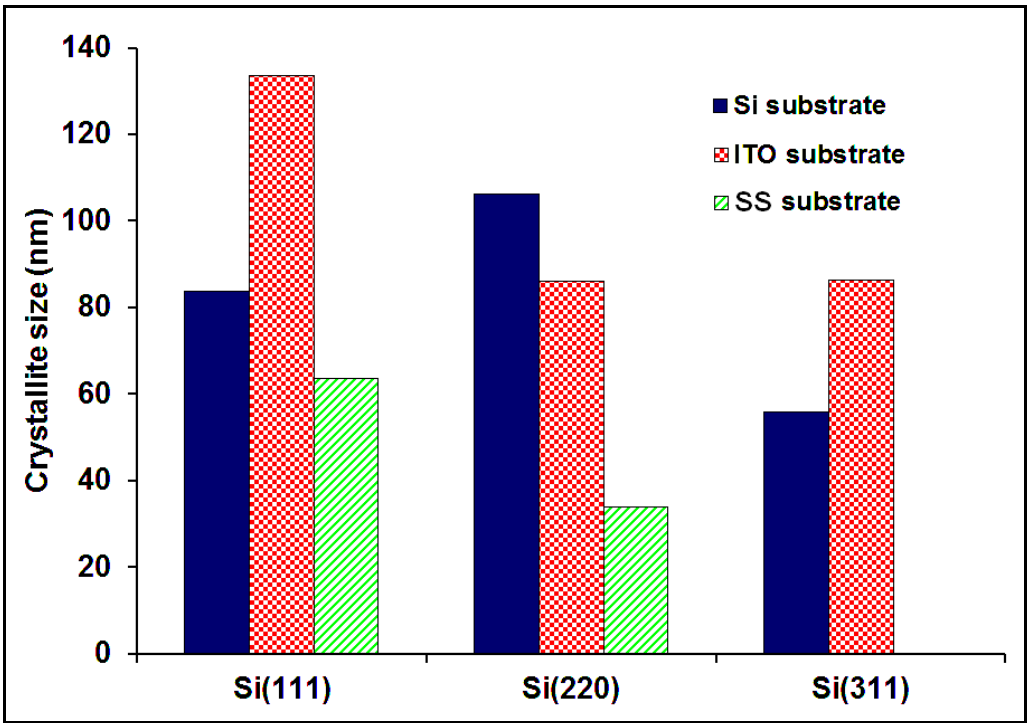
140
120
100
80
60
40
20
0
Crystallite size (nm)
Si substrate
ITO substrate
SS substrate
Si(111)
Si(220)
Si(311)

Fig. 3.

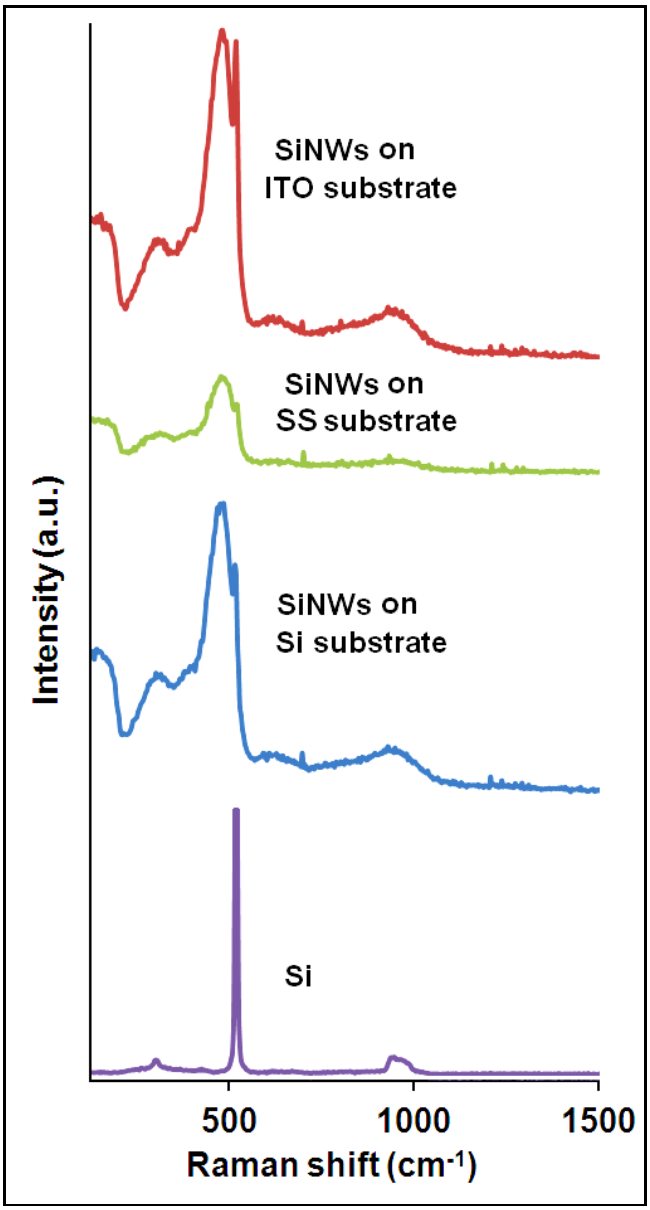
SiNWs on
ITO substrate
SiNWs on
SS substrate
SiNWs on
Si substrate
Si
Intensity (a.u.)
500
1000
1500
Raman shift (cm-1)

Fig. 4.

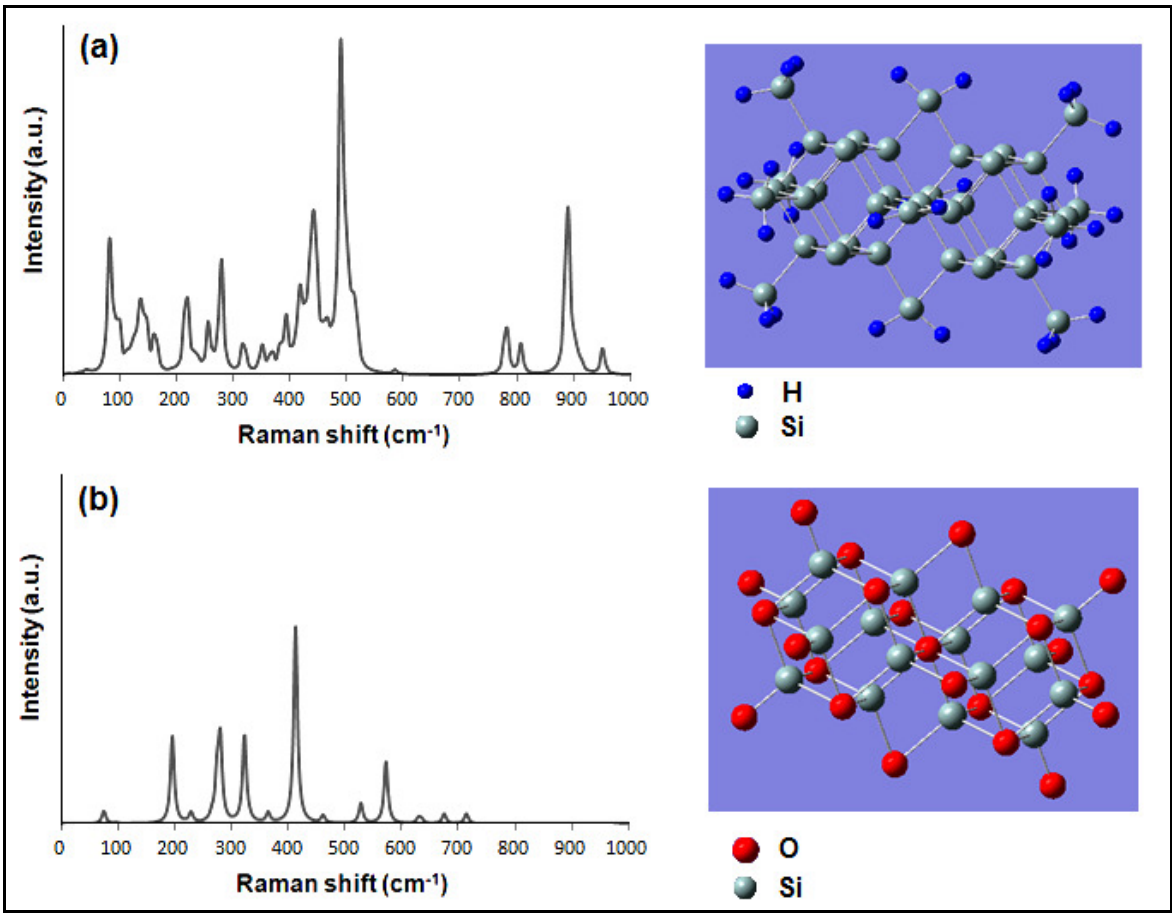
(a)
Intensity (a.u.)
0 100 200 300 400 500 600 700 800 900 1000
Raman shift (cm-1)
H
Si
(b)
Intensity (a.u.)
0 100 200 300 400 500 600 700 800 900 1000
Raman shift (cm-1)
O
Si

Fig. 5.

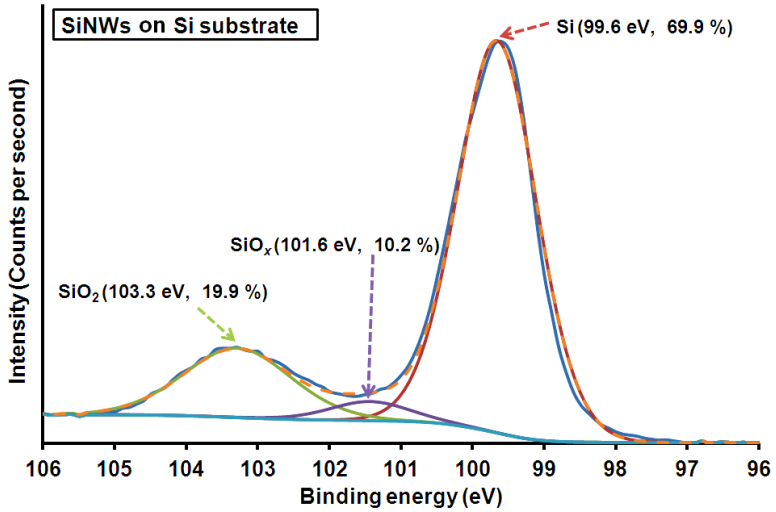
SiNWs on Si substrate
Si (99.6 eV, 69.9 %)
SiOx (101.6 eV, 10.2 %)
SiO2 (103.3 eV, 19.9 %)
Intensity (Counts per second)
106 105 104 103 102 101 100 99 98 97 96
Binding energy (eV)

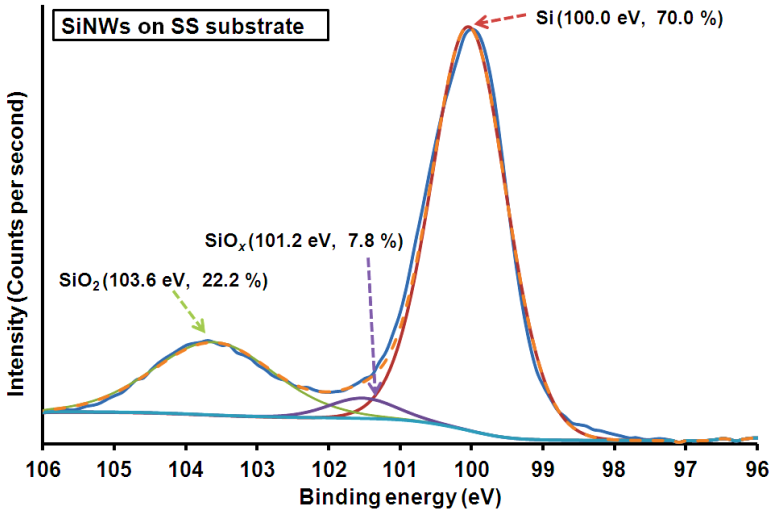
SiNWs on SS substrate
Si (100.0 eV, 70.0 %)
SiOx (101.2 eV, 7.8 %)
SiO2 (103.6 eV, 22.2 %)
Intensity (Counts per second)
106 105 104 103 102 101 100 99 98 97 96
Binding energy (eV)

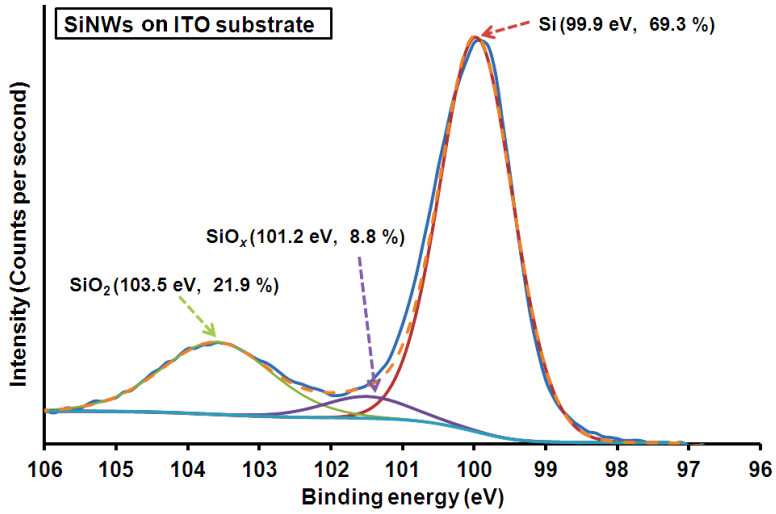
SiNWs on ITO substrate
Si (99.9 eV, 69.3 %)
SiOx (101.2 eV, 8.8 %)
SiO2 (103.5 eV, 21.9 %)
Intensity (Counts per second)
106 105 104 103 102 101 100 99 98 97 96
Binding energy (eV)

Fig. 6.